SUPPORTING INFORMATION

"An In Vivo Model of Ischemic Spinal Cord Injury in Awake Rats Identifies Early Mixed Macrophage Polarization and Impaired Inflammatory Resolution"

[1]Tagore G. de Morais[¶],[1]Caio Perret[¶], [2]Karsten Gronert, [3]Fred A. Lado, [1,4,5]Renato Rozental[*].

SI ILLUSTRATIONS

- 4 SUPPLEMENTARY FIGURES

SUPPORTING INFORMATION
de Morais et al. – Nature Spinal Cord

SI Materials and Methods

Ethics statement. All experimental procedures involving animals and human participants were conducted in accordance with the principles of the Declaration of Helsinki, where applicable, and the National Institutes of Health (NIH) Guide for the Care and Use of Laboratory Animals. The study was reviewed and approved by the respective Institutional Review Boards and Institutional Animal Care and Use Committees (IACUCs). Studies were approved by the Ethics Committees of the Federal University of Rio de Janeiro, Brazil (CAAE 37520820.4.3001.5259) and Hospital Municipal Miguel Couto, Rio de Janeiro, Brazil (CAAE 96263418.0.0000.5279). Animal experiments were approved by the Animal Ethics Committee of the Federal University of Rio de Janeiro (CEUA-UFRJ DAHEICB protocol 053), the Institutional Animal Care and Use Committee of New York Medical College, Valhalla, NY, USA (IACUC protocol 69-12-0609.1), and the Institutional Animal Care and Use Committee of Albert Einstein College of Medicine, Bronx, NY, USA (IACUC protocol 20030906).

Role of the Funders. The funders had no role in the study design; data collection, analysis, or interpretation; manuscript preparation; or the decision to submit the manuscript for publication. The study was conducted independently by the authors, who are solely responsible for the study design, data integrity, interpretation of the findings, and content of the manuscript.

Animals and Experimental Groups

A total of 172 Sprague–Dawley rats were included in the overall experimental program underlying our back-to-back manuscripts: 140 pregnant females subjected to repeated maximal electroshock seizure (MES) stimulation, 20 pregnant control females receiving subthreshold stimulation, and 12 age-matched non-pregnant females subjected to MES stimulation. Animals were 2–3 months old and weighed 200–250 g (Taconic Farms, Germantown, NY, USA). The two manuscripts address complementary phases of the same pathophysiological investigation. Manuscript #1 focuses on the first 24 h after the onset of paralysis, characterizing early inflammatory responses and associated changes in gene expression, protein expression, and histology. Manuscript #2 extends the investigation from the 24-h post-paralysis time point through day 5 after injury to investigate the pathways involved in inflammatory resolution and neuroprotection. Accordingly, the 24-h time point served as a shared temporal reference within the integrated experimental program, linking the characterization of early pathophysiological changes to the subsequent investigation of disease progression and therapeutic intervention. Animals were allocated to the respective experimental groups and analyses according to the objectives and time points of each study.

The pregnant MES-stimulated cohort (n = 140) constituted the primary study group for determining the incidence of persistent paralysis and characterizing

MES-induced ischemic spinal cord injury (SCI). Pregnant control animals (n = 20) underwent identical handling and electrode placement but received subthreshold stimulation (15 V), which did not induce generalized seizures. The age-matched non-pregnant MES-stimulated cohort (n = 12) was included to investigate whether pregnancy-associated physiological adaptations influenced susceptibility to seizure-induced paralysis. These animals were not included in transcriptomic or other molecular gene-expression analyses.

Experimental Design and Sample-Size Rationale.

Rats were selected as the experimental species because ischemic SCI in this model produces prominent tissue macrovacuolization resembling the vacuolar pathology observed in patients. Pregnancy was incorporated into the experimental design because persistent paralysis was not observed in our assays in nonpregnant rats subjected to MES; similarly, persistent paralysis has not been reported in male rats subjected to MES in the published literature. Repetitive tonic seizures induced by MES were used to generate hemodynamic disturbances and watershed ischemia in SC.

No formal *a priori* power calculation was performed. The anticipated incidence of persistent paralysis was approximately 30–35%, based on two complementary lines of evidence. First, anatomical studies demonstrated that the rat SC has a more variable arterial supply than the human SC, and that a single dominant artery equivalent to the human artery of Adamkiewicz is not invariably identifiable[1,2]. This anatomical variability provided a rationale for differential susceptibility to SC ischemia under hemodynamic stress. Second, Isaac and Advokat[3] reported reversible motor paralysis in 35% of rats subjected to repeated transaural electroconvulsive shocks; subsequent work demonstrated that paralysis incidence depended on electrode placement, with transaural stimulation producing paralysis more frequently than transcorneal stimulation[4]. Paraplegia during MES testing was also reported by Bhavsar et al[5]. These findings informed the anticipated incidence as a planning assumption, rather than establishing a direct relationship between arterial anatomy, electroshock exposure, and persistent ischemic paralysis.

In the present protocol, 27.8% of MES-stimulated rats developed persistent paralysis, consistent with the anticipated range. The final cohort size was selected to support characterization of the ischemic SCI model and investigation of the associated inflammatory and neuroprotective mechanisms. Of the 140 pregnant MES-stimulated rats, 40 initially exhibited paralysis; one recovered hindlimb movements within 3 h of the final stimulation and did not meet the criterion for persistent paralysis. The remaining 39 animals constituted the persistent-paralysis cohort. All 39 underwent locomotor assessment at 24 h and the remaining 20 were followed until day 5, comprising 10 untreated animals and 10 treated with 17(S)-HDHA.

The MES-stimulated animals that did not develop paralysis were evaluated in parallel at corresponding time points. Twelve non-paralyzed rats were assessed at 24 h, and an additional 12 were assessed on day 5. At each point, four animals were used for histological analyses, while the remaining animals contributed to molecular biological and functional assessments, as applicable. The specific

analyses performed at each time point, together with the corresponding numbers of animals analyzed, are reported in the Results section.

The pregnant control cohort was divided between 24-h (n = 12) and day-5 (n = 8) assessments. The larger early control cohort supported gene- and protein-expression analyses, while the day-5 cohort provided a time-matched control for the relevant comparisons. Sample sizes therefore varied by outcome and time point according to the experimental protocol and scheduled tissue collection.

MES Stimulation and Seizure Assessment

Transauricular electrical stimulation was delivered through bilateral ear-clip electrodes connected to a constant-voltage stimulator (Grass Instruments, Model S48, Quincy, MA, USA). Animals were briefly restrained for electrode placement and subsequently stimulated while awake. Each stimulation session comprised four consecutive MES stimulations delivered at 30-s intervals. Animals underwent one session during the first experimental week, four sessions during the second week, and seven sessions during the third week.

Generalized tonic–clonic seizures were identified by the characteristic behavioral sequence elicited by MES: tonic flexion, tonic hindlimb extension (THE; bilateral hindlimb extension to approximately 180° relative to the longitudinal body axis), generalized clonic convulsions, and postictal depression. Complete THE or tonic flexion was used as the primary criterion for successful seizure induction. Animals were monitored continuously during each stimulation session and until spontaneous locomotor activity recovered, after which they were returned to their home cages.

Assessment of Transauricular Current and Impedance

Transauricular current was measured under the experimental electrode configuration in seven MES-stimulated no paralyzed animals at the end of the fifth experimental day, immediately after euthanasia. The ear-clip electrodes remained in their original positions, and the stimulation parameters (120 V, 50 Hz, 2 s) were applied while current was measured across the transauricular circuit. Recorded currents ranged from 90 to 137 mA, corresponding to calculated transauricular impedances of 875–1,330 Ω according to Ohm's law. These measurements characterized the current and impedance across the transauricular pathway under the stimulation conditions used in the MES paradigm.

Inclusion and Exclusion Criteria

Inclusion in the persistent-paralysis cohort required paralysis that persisted following MES stimulation. Of the 40 animals initially identified as paralyzed, one recovered hindlimb movements within 3 h of the final stimulation and was excluded from subsequent sampling and analysis because the recovery did not meet the criterion for persistent paralysis. The remaining 39 animals were retained for the planned analyses.

Among the 100 pregnant MES-stimulated animals that did not develop persistent paralysis, MES-associated pregnancy termination occurred in eight animals. These animals were removed from the study and euthanized in accordance with

the approved animal-welfare protocol; they were excluded from subsequent analyses. Animal numbers contributing to individual outcomes are reported in the corresponding Results sections.

Randomization and Blinding

Within the relevant experimental groups, animals were randomly selected for electromyographic, magnetic resonance imaging (MRI), and X-ray assessments, as applicable to the experimental protocol. Seven MES-stimulated animals were also selected for transauricular current and impedance measurements. This selection determined which animals underwent particular assessments and was distinct from random allocation to treatment groups.

Behavioral assessments of control animals and MES-stimulated animals that did not develop paralysis were performed under blind conditions. Animals developing paralysis were identified by direct visual observation to enable timely assessment; therefore, identification of paralysis itself was not blinded. Among animals with paralysis, allocation of 17(S)-HDHA treatment or the untreated group was randomized. Histological quantification and transcriptomic and proteomic analyses were performed by investigators blinded to experimental group for the animals included in the respective analyses. MRI and electromyographic (EMG) assessments were not blinded to investigators.

Humane Endpoints, Animal Monitoring, and Welfare

Animals were monitored daily for general health and well-being, including access to and the ability to consume food and water, spontaneous locomotor activity, behavioral changes, signs of pain or distress, and vaginal bleeding in pregnant rats. Monitoring also included assessment of spontaneous locomotor recovery following MES stimulation. Animals exhibiting severe or persistent distress, inability to eat or drink, or other signs of significant deterioration were to be euthanized in accordance with the approved institutional animal-care and ethics protocols. These procedures were intended to minimize animal suffering and ensure compliance with applicable animal-welfare standards.

Persistent hindlimb paralysis following MES stimulation was the principal expected experimental outcome. Pregnancy termination in eight non-paralyzed MES-stimulated animals was an additional adverse event. These animals were euthanized and excluded from subsequent analyses in accordance with the approved welfare protocol.

Housing, Husbandry, and Ethical Approval

Animal care and husbandry followed applicable institutional policies at Albert Einstein College of Medicine (New York, NY, USA), New York Medical College (Valhalla, NY, USA), and Universidade Federal do Rio de Janeiro (Rio de Janeiro, Brazil), together with applicable animal-welfare regulations and the *Guide for the Care and Use of Laboratory Animals*. Protocol-specific procedures, including the use of pregnant animals and awake, unanesthetized MES stimulation, were approved by the relevant institutional animal-care and ethics committees.

Pregnancy was an integral component of the experimental model. The use of awake animals avoided potential confounding effects of anesthetic agents on

seizure induction and injury development. Animals were housed individually under controlled light–dark cycles and received veterinary care throughout the study.

Data Availability

The microarray dataset is publicly available through the Gene Expression Omnibus (GEO) under accession number GSE345827. Data supporting the other findings, including histological, biochemical, X-ray, MRI, and functional data, are available from R.R. (Fiocruz) upon reasonable request. Rat cerebrospinal-fluid (CSF) lipidomics and *Alox15* data are available from K.G. (University of California, Berkeley). Human CSF lipidomics data and measurements of deuterium-labeled 17(S)-HDHA in rats are available from F.C.S.N. (Universidade Federal do Rio de Janeiro) upon reasonable request and subject to applicable ethical and data-sharing restrictions.

Tissue collection, RNA extraction, microarray processing, and transcriptomic analysis. At 24 h after the onset of paralysis, nine independent biological samples were collected for transcriptomic analysis, comprising three uninjured control animals, three MES-stimulated animals that did not develop paralysis, and three MES-stimulated animals that developed persistent paralysis. The MES-stimulated groups were time-matched. Animals were deeply anesthetized and euthanized, and the thoracic SC segments spanning T8–T12, encompassing the T10 lesion epicenter, were rapidly dissected under RNase-free conditions. Tissue collection was completed within 3–5 min of euthanasia to minimize RNA degradation. Each specimen was immediately transferred to a sterile RNase-free cryovial, snap-frozen in liquid nitrogen, and stored at −80 °C. Samples were maintained continuously at −80 °C and transported on dry ice to Genome Explorations (Memphis, TN, USA) without freeze–thaw cycles.

Total RNA was extracted by Genome Explorations using standardized procedures optimized for neural tissue. RNA concentration and purity were assessed spectrophotometrically by measuring A260/A280 and A260/A230 ratios. RNA integrity was evaluated using microfluidic capillary electrophoresis with an Agilent 2100 Bioanalyzer (Agilent Technologies, Santa Clara, CA, USA). Samples with an RNA Integrity Number (RIN) ≥8.0 were considered suitable for downstream microarray analysis. Representative RNA quality-control profiles are shown in **Supplementary Fig. 3.**

Affymetrix microarray processing. High-quality RNA samples were processed for genome-wide expression profiling using Affymetrix Rat Genome 230 2.0 arrays according to the manufacturer's recommended procedures. Briefly, RNA was reverse-transcribed and amplified, and the resulting labeled complementary RNA was hybridized to the arrays. Following hybridization, arrays were washed, stained, and scanned using the manufacturer's recommended instrumentation. Raw fluorescence intensity data were exported as CEL files for downstream computational analysis.

Microarray data preprocessing and normalization. CEL files were imported into R using the Bioconductor affy package. Because the Affymetrix Rat Genome 230 2.0 platform contains paired perfect-match (PM) and mismatch (MM) probes, the

Microarray Suite 5.0 (MAS 5.0; Affymetrix) algorithm was used for probe-level background correction and probe-set summarization. MAS 5.0 processing also generated detection calls (Present, Marginal, or Absent), which were used to assess the repertoire of detectably expressed transcripts. Processed expression values were $\log_2$-transformed prior to downstream statistical analysis. Probe-set annotations were assigned using the rat2302.db Bioconductor annotation package.

Differential gene-expression analysis. Differential expressions were assessed using the limma package in R. Comparisons were performed among the three experimental groups, with particular emphasis on the contrasts between paralyzed animals and uninjured controls and between paralyzed and MES-stimulated non-paralyzed animals. Linear models were fitted to the normalized expression data, and empirical Bayes moderation was applied to the estimated variances. Multiple-testing correction was performed using the Benjamini–Hochberg procedure.

Genes were considered differentially expressed when they met both criteria of an adjusted *P* value <0.05 and an absolute $\log_2$ fold-change ≥ I1I. Differentially expressed genes were subsequently used for cellular-signature and pathway analyses described in the main text.

Biological pathway and gene-expression analysis. To characterize the biological processes associated with the transcriptional response to ischemic SCI, DEGs identified at 24 h were subjected to functional annotation and pathway-enrichment analyses. GO analysis was used to identify enriched biological processes, molecular functions, and cellular components, whereas KEGG and Reactome analyses were used to identify enriched signaling, metabolic, and cellular pathways. Analyses were performed using the Enrichr platform together with complementary gene-set enrichment approaches, and statistical significance was assessed using appropriate multiple-testing correction.

In addition to database-driven enrichment, pathway-level findings were examined within a literature-guided biological framework focused on processes known to contribute to the acute response to ischemic SCI. These included inflammatory signaling and innate immune activation, monocyte/macrophage recruitment and differentiation, astrocytic and microglial responses, lipid and fatty-acid metabolism, neuronal and axonal responses, and extracellular-matrix remodeling. These categories were used to facilitate biological interpretation of the enriched pathways rather than as independent statistical classifications.

Reactome analysis of highly upregulated transcripts. The 50 most strongly upregulated genes were examined individually and mapped to Reactome pathways to identify biological processes disproportionately represented among the most prominent transcriptional changes. Particular attention was given to immune-related pathways and genes associated with macrophage phenotypes, including Arg1, as well as pathways involved in circulating monocyte differentiation and resolution-associated programs linked to docosahexaenoic acid (DHA) metabolism.

Finally, pathway-level results were integrated with individual-gene expression patterns and with the biochemical, histological, and inflammatory findings obtained at the same 24-h time point. This integrative approach enabled interpretation of the transcriptomic response at both the individual-gene and biological-pathway levels, reducing reliance on isolated transcript changes and providing a framework for linking molecular alterations to the cellular and tissue responses observed after ischemic SCI.

Data deposition. The complete microarray dataset, including the raw CEL files and processed expression data, was deposited in the NCBI Gene Expression Omnibus (GEO) database in accordance with MIAME recommendations. The GEO accession number is provided in the Data Availability statement.

Real-Time Quantitative PCR (RT-qPCR). RNA was isolated from SC samples obtained from three control and three paralyzed animals using TRIzol reagent (Invitrogen, Carlsbad, CA, USA) and from primary cultured astrocytes using the Absolute RNA® Miniprep Kit (Stratagene, La Jolla, CA, USA). Astrocyte experiments comprised three independent experiments, with two replicates per condition. RNA integrity was assessed by agarose gel electrophoresis, and RNA concentration was determined spectrophotometrically. RNA was reverse-transcribed using the SuperScript III First-Strand Synthesis System (Invitrogen). Rat leukocyte 12/15-LOX (Alox15) was amplified using established nucleotide primers[6]; sense 5'-GGCCCCGGAGACCAAGGAT-3' and antisense 5'-GCCGCCGCCACATTCAGG-3'. Specific nucleotide primers for rat reference genes (ubiquitin C, GAPDH, β-actin) were selected from the Real-Time PCR Data Base (medgen.ugent.be/rtprimerdb) and verified in the NIH Genbank®: Real-time PCR was performed using Brilliant SYBR Green QPCR Master Mix (Stratagene) and an MX3000 QPCR System (Stratagene). All amplifications were run in duplicates and amplification efficiencies for each primer pair were established. Comparative quantitation of gene expression was determined by MXPro analytical software (Stratagene).

SearchLight multiplex cytokine and chemokine assay. SC tissue samples were collected separately from the T8, T10, and T12 levels from three experimental groups: uninjured controls, MES-stimulated animals without paralysis, and MES-stimulated animals with persistent paralysis (n = 3 animals per group). Tissue homogenates were analyzed using the SearchLight® Multiplex Protein Array platform (Pierce Biotechnology, Inc., Woburn, MA, USA). The assay uses a multiplexed sandwich ELISA format in which analyte-specific capture antibodies are arrayed within individual wells. Following incubation with tissue homogenates, bound proteins were detected using biotinylated detection antibodies and streptavidin–horseradish peroxidase, followed by chemiluminescent detection using the SearchLight imaging system. Concentrations were determined from analyte-specific standard curves. The panel comprised Fractalkine (CX3CL1), GRO/KC (CXCL1), MCP-1 (CCL2), MIP-2 (CXCL2), RANTES (CCL5), IL-1β, IL-4, IL-6, and TNF-α. Each sample was analyzed in duplicate; the mean of the duplicate measurements was calculated and corrected for the corresponding sample dilution. Final concentrations were

expressed as pg/mL. Statistical analysis were performed using ANOVA on Jamovi Software (2.6 version)[7] following concentrations log10 transformation.

X-ray and magnetic resonance imaging. Spinal radiographs were obtained from five paralyzed rats at Jacobi Medical Center, Albert Einstein College of Medicine, Bronx, NY, USA, using a Siemens Medical Systems conventional radiography system and standard clinical radiographic techniques. Imaging was performed 24 h after paralysis in three animals and on day 5 in two animals. Magnetic resonance imaging (MRI) was performed in two paralyzed rats at the Gruss Magnetic Resonance Research Center (MRRC), Albert Einstein College of Medicine, Bronx, NY, USA, using a 9.4-T Varian animal MRI/MRS system with a 21-cm bore. MRI and radiographic assessments were performed by investigators who were not blinded to experimental group. The system was designed for high-field small-animal anatomical imaging and spectroscopy and included dedicated rodent radiofrequency coils and high-performance gradient/shim hardware. T2-weighted multislice spin-echo images were acquired from the brain and SC with repetition time (TR) = 1.5 s, echo time (TE) = 40 ms, and 1-mm slice thickness**.** Images were obtained on day 5 after the onset of MES-induced paralysis for anatomical characterization of the lesion[8]. The use of this high-field platform for experimental rat MRI/MRS at Einstein has been previously reported[9,10]**.**

Study Locations and Experimental Procedures. Experimental procedures were conducted at the academic research laboratories and animal facilities, where maximal electroshock seizure (MES) stimulation and associated animal assessments were performed, and at Genome Explorations, Inc., where gene-expression analyses were conducted.

SI REFERENCES

1. Tveten L. Spinal cord vascularity. IV. The spinal cord arteries in the rat. *Acta Radiol Diagn (Stockh)*. **17(4)**, 385-98 (1976)
2. Schievink WI, Luyendijk W, Los JA. Does the artery of Adamkiewicz exist in the albino rat? *J. Anat.* **161**, 95-101 (1988).
3. Isaac L, Advokat C. Reversible motor paralysis in rats after repeated electroconvulsive shock. *Exp Neurol*. **85 (1)**, 87-96 (1984).
4. Isaac L, Advokat C, Nelson DK, Browning RA. Motor paralysis in rats after repeated electroconvulsive shock: comparison between aural and corneal stimulation. *Life Sci*. **37(13),** 1257-64 (1985).
5. Bhavsar VH, Batham AK, Saifi AQ. Paraplegia observed during maximal electroshock seizure test in rats. *Indian J Med Res*. **65(5)**, 734-7 (1977).
6. Nigam, S., Fiore, S., Luscinskas, F. W. & Serhan, C. N. The rat leukocyte-type 12-lipoxygenase exhibits an intrinsic hepoxilin A3 synthase activity. *J. Biol. Chem.* **279**, 29023–29030 (2004).
7. The jamovi project. jamovi (**Version 2.7**) https://www.jamovi.org (2026).
8. Felder J, Celik AA, Choi CH, Schwan S, Shah NJ. 9.4 T small animal MRI using clinical components for direct translational studies**.** *J Transl Med*. **15 (1)**, 264 (2017).

9. Miyasaka N, Takahashi K, Hetherington HP. Fully automated shim mapping method for spectroscopic imaging of the mouse brain at 9.4 T. *Magn Reson Med***. 55**,198–202 (2006).
10. Gomes WA, Lado FA, de Lanerolle NC, Takahashi K, Pan C, Hetherington HP. Spectroscopic imaging of the pilocarpine model of human epilepsy suggests that early NAA reduction predicts epilepsy. *Magn Reson Med***. 58** (2), 230–235 (2007).
11. Pfaffl MW. A new mathematical model for relative quantification in real-time RT-PCR. *Nucleic Acids Res.* **29(9):**e45 (2001).

SUPPLEMENTARY FIGURES

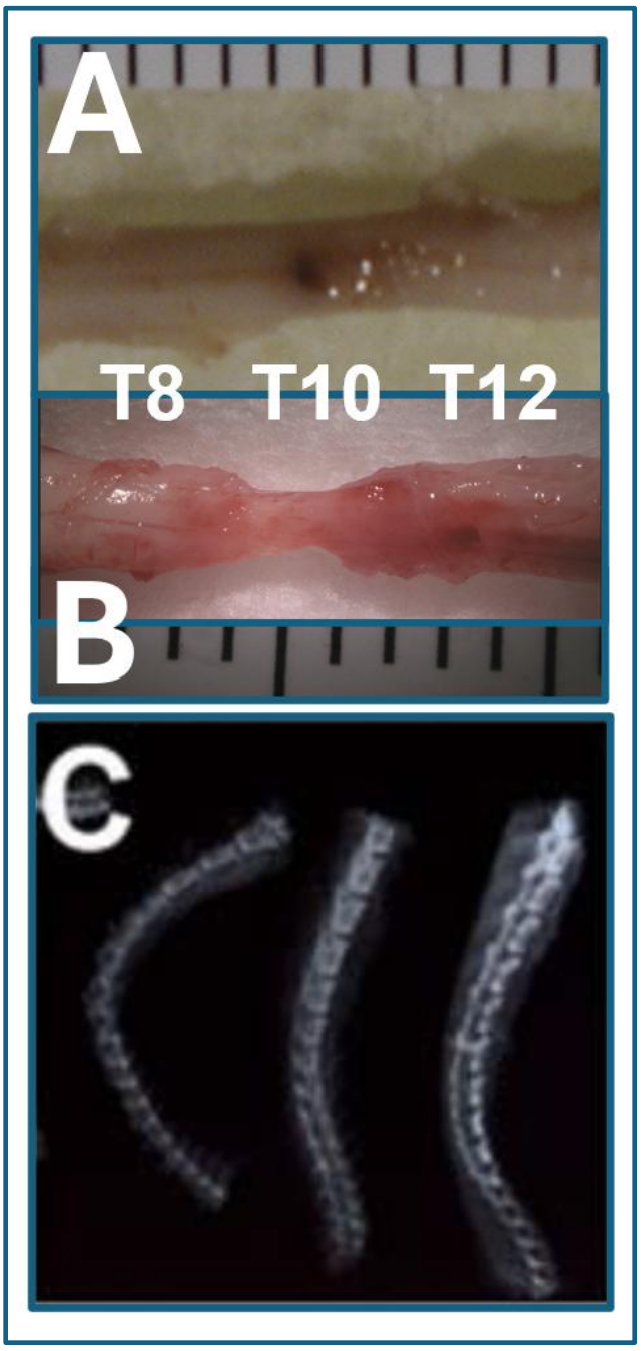

Fig. S1. Structural and radiographic characterization of spinal cord injury after MES. (A) Representative SC at 24 h after paralysis, showing focal hemorrhage and inflammatory changes during the hyperacute phase. **(B)** At 5 days, marked tissue degeneration and loss were evident at the lesion epicenter (T10), with greater involvement at T12 than T8. **(C)** X-ray radiography in 5 stimulated rats showed no vertebral fracture, despite the intense muscle contractions induced by MES, supporting the non-traumatic, ischemic nature of the SCI produced by this protocol.

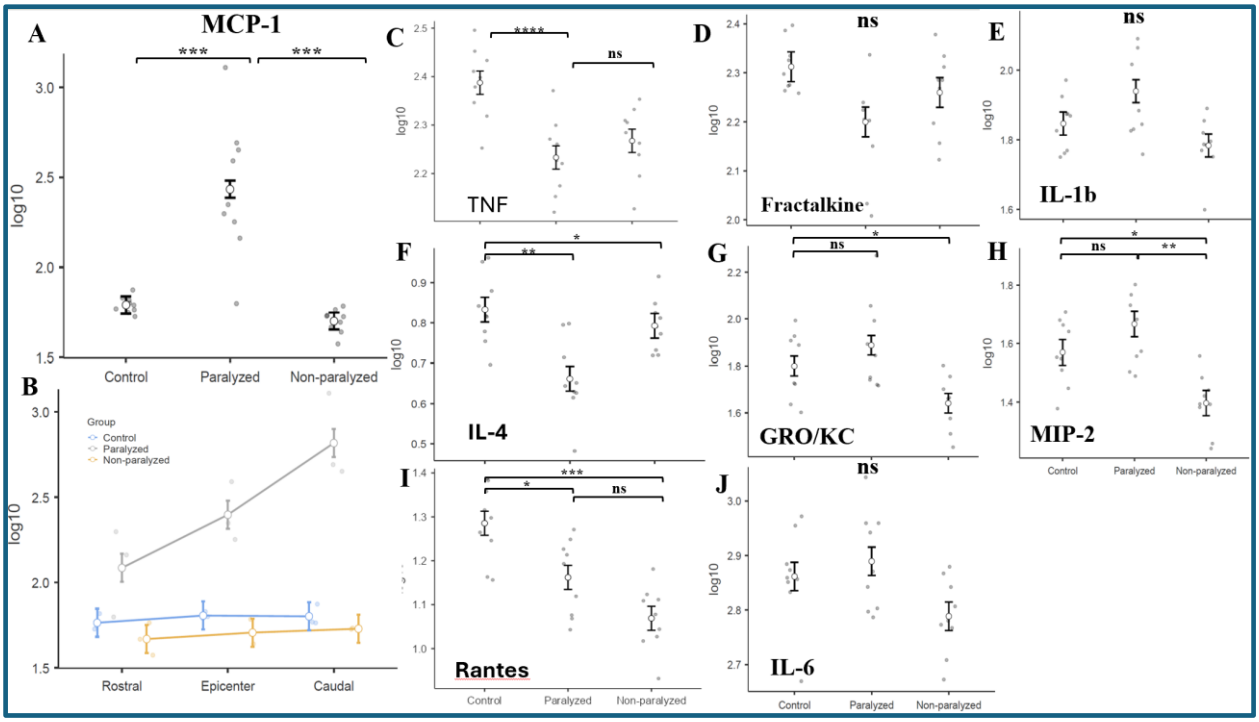

Fig. S2. Regional cytokine and chemokine profiling in acute spinal cord injury. (A–J) Nine cytokines and chemokines previously reported in experimental SCI models and patients were quantified in T8, T10, and T12 SC homogenates 24 h after paralysis using a 9-plex SearchLight® protein array (n = 3 per group). MCP-1/CCL2 showed the most prominent increase, with other mediators displaying regional modulation. The profile supports a temporally and molecularly selective inflammatory response, characterized at 24 h by MCP-1-associated myeloid recruitment and selective suppression/remodeling of cytokine programs, rather than a generalized cytokine surge. Values represent duplicate measurements corrected for sample dilution and expressed as pg/mL. Statistical analysis were performed using ANOVA on Jamovi Software (2.6 version)[7] following concentrations log10 transformation.

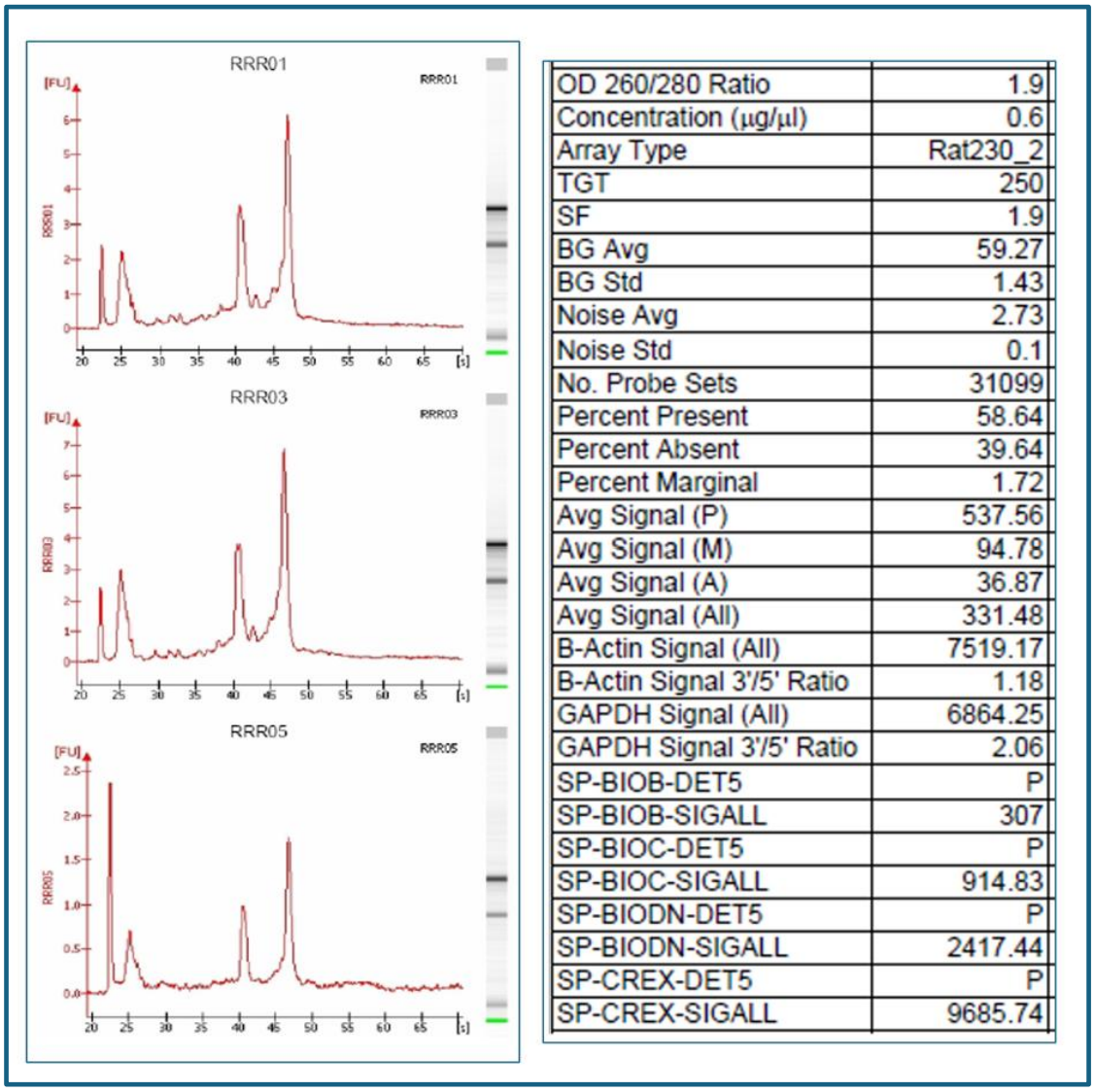

OD 260/280 Ratio	1.9
Concentration (μg/μl)	0.6
Array Type	Rat230_2
TGT	250
SF	1.9
BG Avg	59.27
BG Std	1.43
Noise Avg	2.73
Noise Std	0.1
No. Probe Sets	31099
Percent Present	58.64
Percent Absent	39.64
Percent Marginal	1.72
Avg Signal (P)	537.56
Avg Signal (M)	94.78
Avg Signal (A)	36.87
Avg Signal (All)	331.48
B-Actin Signal (All)	7519.17
B-Actin Signal 3'/5' Ratio	1.18
GAPDH Signal (All)	6864.25
GAPDH Signal 3'/5' Ratio	2.06
SP-BIOB-DET5	P
SP-BIOB-SIGALL	307
SP-BIOC-DET5	P
SP-BIOC-SIGALL	914.83
SP-BIODN-DET5	P
SP-BIODN-SIGALL	2417.44
SP-CREX-DET5	P
SP-CREX-SIGALL	9685.74

Fig. S3. RNA quality assessment of spinal cord samples used for microarray analysis. Representative RNA electropherograms generated by Genome Explorations, Inc. (Memphis, TN, USA) from T10 SC tissue collected 24 h after the onset of paralysis from stimulated paralyzed rats, together with samples collected at the corresponding time point from MES-stimulated non-paralyzed rats and uninjured control animals (bottom to top). All samples displayed the characteristic RNA profile with two prominent ribosomal RNA peaks, with the first peak located at approximately 40 s and the second between 45 and 50 s, consistent with preserved RNA integrity and suitable quality for downstream microarray analysis. The corresponding RNA quality-control summary provided by the analysis software is shown on the right and includes optical density (OD) measurements, RNA concentration, array type, average signal (AVG), and noise for each sample. Samples meeting predefined quality criteria were accepted for downstream transcriptomic analysis.

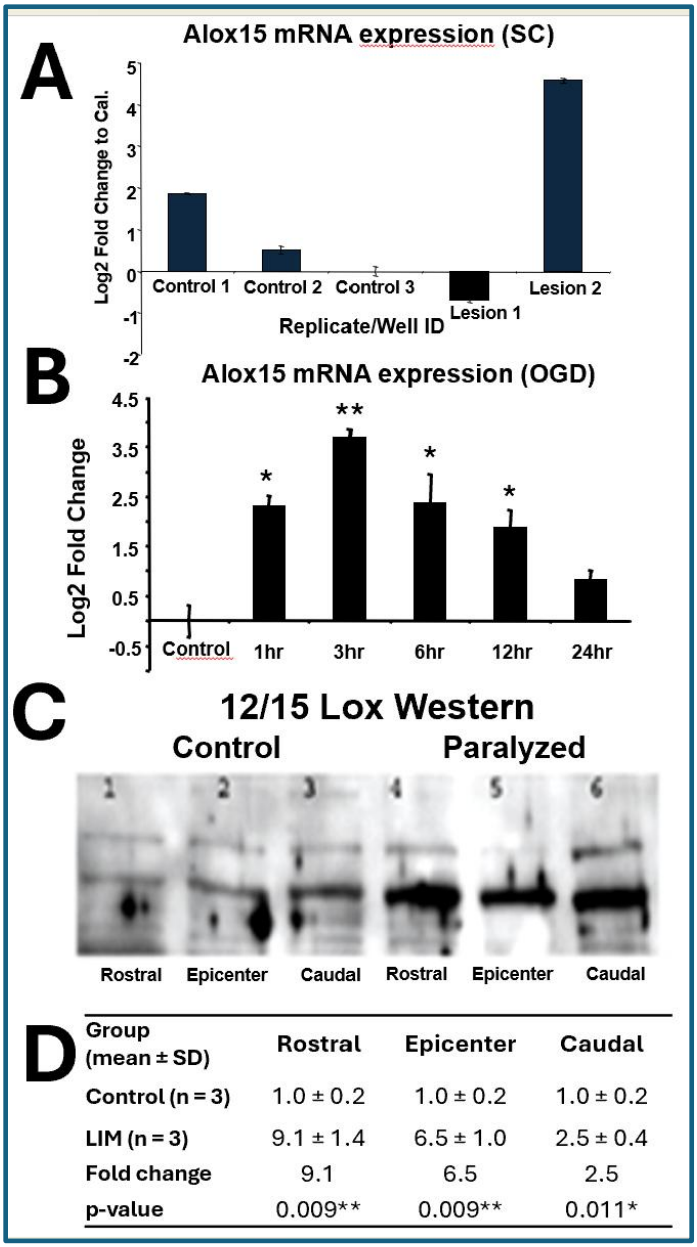

Group (mean ± SD)	Rostral	Epicenter	Caudal
Control (n = 3)	1.0 ± 0.2	1.0 ± 0.2	1.0 ± 0.2
LIM (n = 3)	9.1 ± 1.4	6.5 ± 1.0	2.5 ± 0.4
Fold change	9.1	6.5	2.5
p-value	0.009**	0.009**	0.011*

Fig. S4. Temporal regulation of *Alox15* expression and 12/15-LOX protein after ischemic-like stress and spinal cord injury. (**A**) *Alox15* mRNA expression in spinal cord (SC) tissue at 12 and 24 h after paralysis. A transient approximately fourfold increase was observed at 12 h, followed by reduced expression at 24 h. Data are expressed as log fold change after normalization to *UBC* using the Pfaffl method (2001)[11]. (**B**) *Alox15* mRNA expression in primary rat SC astrocytes subjected to oxygen–glucose deprivation (OGD). *Alox15* expression increased transiently during the first 3 h of OGD and subsequently returned toward baseline by 24 h. Data are from three independent experiments, with two technical replicates per condition, normalized to *UBC* and expressed as fold change relative to normoxic controls. $P < 0.05$ versus normoxic controls (one-way ANOVA). (**C**) Representative immunoblot showing 12/15-lipoxygenase (12/15-LOX) protein expression in SC tissue at day 5 after paralysis, with the corresponding loading control. (**D**) Densitometric quantification of 12/15-LOX protein expression in SC tissue at day 5 after paralysis.